

# Adsorption of metal atoms at a buckled graphene grain boundary using model potentials

Edit E. Helgee<sup>1</sup> and Andreas Isacson<sup>1</sup>

Department of Applied Physics, Chalmers University of Technology, SE-412 96, Göteborg, Sweden

Two model potentials have been evaluated with regard to their ability to model adsorption of single metal atoms on a buckled graphene grain boundary. One of the potentials is a Lennard-Jones potential parametrized for gold and carbon, while the other is a bond-order potential parametrized for the interaction between carbon and platinum. Metals are expected to adsorb more strongly to grain boundaries than to pristine graphene due to their enhanced adsorption at point defects resembling those that constitute the grain boundary. Of the two potentials considered here, only the bond-order potential reproduces this behaviour and predicts the energy of the adsorbate to be about 0.8 eV lower at the grain boundary than on pristine graphene. The Lennard-Jones potential predicts no significant difference in energy between adsorbates at the boundary and on pristine graphene. These results indicate that the Lennard-Jones potential is not suitable for studies of metal adsorption on defects in graphene, and that bond-order potentials are preferable.

## I. INTRODUCTION

The two-dimensional carbon material graphene is frequently considered for sensors, electronics and catalysis applications due to its exceptional electric and mechanical properties<sup>1</sup>. Some of these applications require the adsorption of metal clusters onto graphene, and metal-graphene systems have consequently become a subject of intense investigation. For computational studies of metal adsorption on graphene, *ab initio* methods such as density functional theory give the most accurate description of the metal-carbon interaction. However, *ab initio* methods are computationally expensive. For problems requiring simulations of large systems it can therefore be necessary to make use of interatomic model potentials.

One problem that may require the use of interatomic model potentials is that of adsorption at graphene grain boundaries. Grain boundaries are common in CVD-grown graphene<sup>2,3</sup> and have lately received attention due to their influence on both the electronic and mechanical properties of the material<sup>4</sup>. The grain boundaries are known to consist of arrays of dislocations in the form of pentagon-heptagon defect pairs and to cause out-of-plane buckling<sup>5–8</sup>. Interestingly, graphene grain boundaries have been found to be more chemically reactive than pristine graphene<sup>9</sup>.

Among the existing model potentials for the interaction between metals and carbon, two types of potentials appear to be common. One is the Lennard-Jones potential, a simple pair potential modelling van der Waals attraction, which is often used for gold adsorbates. The other category is bond-order potentials, a potential type that was originally developed for covalently bonded solids<sup>13,14</sup> but which has been found to be able to describe also metal-semiconductor interactions<sup>15</sup>. The question is to what extent these two potential types are reliable, in particular with regard to adsorption on grain boundaries.

Here, we investigate the adsorption of single metal atoms on pristine graphene and a buckled graphene grain boundary using two different model potentials for the carbon-adsorbate interaction. One of the potentials is a bond-order potential for carbon and platinum, while the other is

the Lennard-Jones pair potential with potential parameters chosen to describe the interaction of carbon and gold. As the Lennard-Jones potential is a very simple, it is unlikely that it gives a good description of the adsorption of gold on defects in graphene. However, it is quite common to use the Lennard-Jones potential to describe the adsorption of gold on graphene (see *e.g.* Refs. 10–12), and an investigation of the applicability of this potential to the present problem is therefore motivated.

The results for pristine graphene are compared to density functional theory results available in the literature<sup>30,31</sup>. To the best of our knowledge there are no previous studies of metal adsorption on graphene grain boundaries, but several density functional theory studies<sup>16–20</sup> suggest that metals adsorb more strongly to pentagon and heptagon defects than to pristine graphene. Computational studies also indicate that gold and platinum adsorb more strongly to curved graphene surfaces than to flat graphene<sup>21,22</sup>. As grain boundaries consist of a line of pentagon-heptagon defects and cause the graphene to buckle, this indicates that metals should adsorb more strongly to grain boundaries than to pristine graphene.

For pristine graphene, both potentials are found to produce adsorption energies similar to those seen in DFT studies for the most favourable adsorption site, although the bond-order potential predicts considerably weaker adsorption at other adsorption sites. At the buckled grain boundary, the Lennard-Jones potential predicts no substantial increase in adsorption strength, while the bond-order potential finds an increase in adsorption strength of 0.8 eV. The bond-order potential also reproduces the expected behavior with regard to the curvature of the graphene sheet. This implies that results obtained with the Lennard-Jones potential are misleading for graphene with grain boundaries, and that bond-order potentials are preferable in such cases.

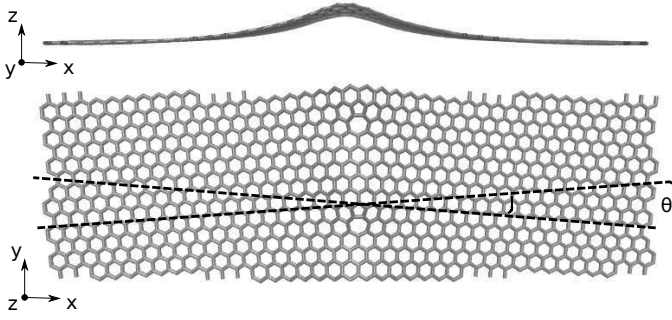


Figure 1. (Color online) Grain boundary with misorientation angle  $9.4^\circ$ , seen from the  $y$  direction (top) and from the  $z$  direction (bottom). Figure created using VMD<sup>29</sup>.

## II. METHOD

All modelling has been performed using the program package LAMMPS<sup>23</sup>. Structure optimizations have been carried out using a conjugate gradients energy minimization algorithm and the size and shape of the system were allowed to change during the minimization process.

In the simulations of adsorption of gold on graphene, the carbon-carbon interaction is modeled by a modified Tersoff potential<sup>14</sup>. This potential has been adapted by Lindsay and Broido<sup>24</sup> to better reproduce the phonon dispersion in graphene, and it was chosen in order to facilitate prospective studies of the effects of adsorbates on vibrational properties. The gold-carbon interaction was described by a Lennard-Jones potential, using a set of potential parameters that have previously been used in Ref.<sup>10</sup> ( $\epsilon_{\text{Au-C}} = 0.0341$  eV,  $\sigma_{\text{Au-C}} = 3.003$  Å).

For the interaction between platinum and carbon, a bond-order potential developed by Albe et al. has been used<sup>15</sup>. This potential builds on the reactive bond-order potential (REBO) by Brenner et al.<sup>25,26</sup>. The potential has previously been used *e.g.* to investigate the adsorption of platinum clusters at vacancies in graphene<sup>27</sup>.

For adsorption of atoms on pristine graphene a  $5 \times 5$  nm graphene sheet was used. It was ascertained that using a larger graphene sheet did not appreciably change the results. For the investigations of adsorption on grain boundaries a tilt grain boundary with misorientation angle  $9.4^\circ$  has been studied (see Fig. 1). This grain boundary consists of pentagon and heptagon defects and displays a buckling approximately 0.6 nm high and 1.7 nm wide. The process of grain boundary construction and the properties of the grain boundary are described in Ref.<sup>28</sup>. A grain boundary supercell 20 nm long in the direction perpendicular to the grain boundary ( $x$ ) and 4.5 nm long in the direction parallel to the grain boundary ( $y$ ) was used, corresponding to three grain boundary periods in the  $y$  direction.

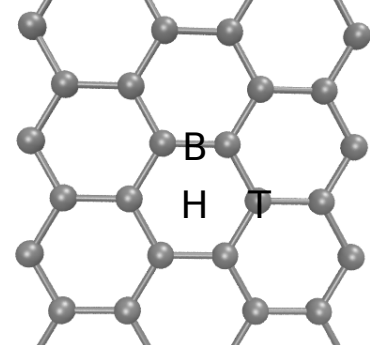


Figure 2. Adsorption positions hexagon (H), top (T) and bridge (B) for a single atom on pristine graphene. Figure created using VMD<sup>29</sup>.

## III. RESULTS

The adsorption energy for an atom on graphene is defined as

$$E_a = E_{\text{tot}} - E_G, \quad (1)$$

where  $E_{\text{tot}}$  is the total energy of the graphene sheet with the adsorbed atom and  $E_G$  is the energy of the graphene sheet without adsorbate. With this definition, a negative adsorption energy means that the adsorption is favoured, as it lowers the total energy.

Three adsorption positions have been considered for single atoms on pristine graphene: top (T), bridge (B) and hexagon (H) (see Figure 2). With the Lennard-Jones potential for gold, the hexagon position has the largest adsorption energy,  $-0.45$  eV, while the top and bridge positions have adsorption energies of  $-0.42$  and  $-0.43$  eV, respectively. These results compare fairly well with the DFT results for gold atoms obtained by Amft et al.<sup>30</sup>, who found adsorption energies between  $-0.3$  and  $-0.9$  eV when using functionals that take van der Waals interactions into account. However, DFT calculations predict the top adsorption position, rather than the hexagon position, as the position with the most negative segregation energy.

With the bond-order potential for the carbon-platinum system, the adsorbed atom is found to be most stable in the bridge position, where the adsorption energy is  $-1.93$  eV. For the hexagonal position the adsorption energy was  $-0.08$  eV, while for the top position it was found to be  $0.23$  eV. Density functional calculations for platinum adsorbates<sup>31</sup> have yielded adsorption energies near  $-2$  eV for the bridge position,  $-1.4$  eV for the hexagon position and  $-1.9$  eV for the top position. The interatomic potential and density functional theory thus predict the same site as the most favourable adsorption site, but for the other two adsorption sites the interatomic potential predicts weak or no adsorption, in contrast to the density functional theory results. This suggests that the potential in use here may be adequate for studies of static adsorbates, but not for studies involving *e.g.* diffusion.

Several different adsorption sites were considered for the

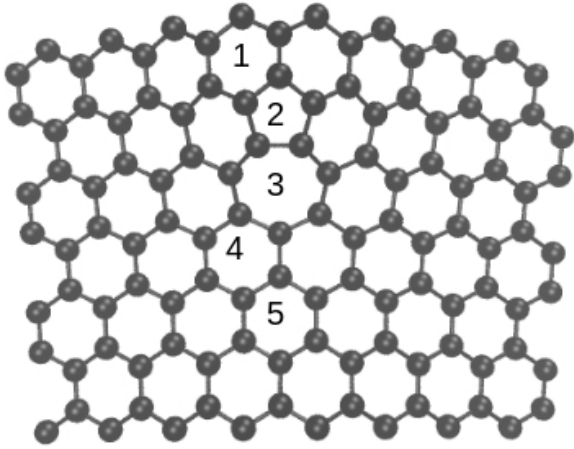


Figure 3. Adsorption positions for a gold atom on a graphene grain boundary. Figure created using VMD<sup>29</sup>.

Table I. Adsorption energies for a gold atom adsorbed at the grain boundary, above and below the graphene sheet. The site numbers correspond to the adsorption positions labeled in Figure 3

Site	$E_a$ (eV) (above)	$E_a$ (eV) (below)
1	-0.06	-0.49
2	-0.01	-0.50
3	-0.16	-0.32
4	0.17	-0.27
5	-0.22	-0.20

grain boundary, as can be seen in Figures 3 and 4. For gold, only adsorbate positions in the middle of hexagons, heptagons or pentagons were considered since the hexagon position was found to be the most stable on pristine graphene. Likewise, only adsorption sites between two carbon atoms were considered for platinum. Due to the buckling of the grain boundary it was also necessary to consider adsorption on both sides of the graphene sheet. Referring to the coordinate systems defined in Figure 1, adsorption sites where the adsorbate has a higher  $z$  coordinate than the graphene sheet will be denoted "above" sites and adsorption sites where the adsorbate has a lower  $z$  coordinate than the sheet will be denoted "below" sites.

The obtained adsorption energies for gold atoms range from  $-0.5$  to  $0.17$  eV, as can be seen in Table I. The largest negative adsorption energies are found below the peak of the grain boundary buckle, position 2 in Figure 3. This is probably due to the simple pair potential used to describe the gold-carbon interaction favoring configurations where the adsorbate has many nearest neighbours. An adsorbate under the buckle is relatively close to a larger number of carbon atoms compared to flat graphene, while on top of the buckle the graphene curves away from the adsorbate, giving fewer nearest neighbours and smaller adsorption energies.

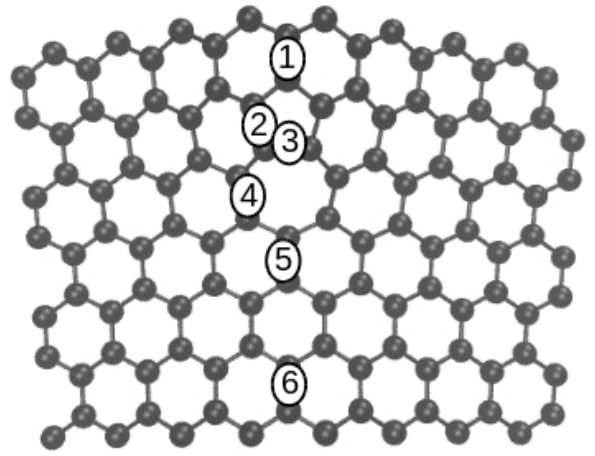


Figure 4. Adsorption positions for a platinum atom on a graphene grain boundary. Figure created using VMD<sup>29</sup>.

Table II. Adsorption energies for a platinum atom adsorbed at the grain boundary, above and below the graphene sheet. The site numbers correspond to the adsorption positions labeled in Figure 4

Site	$E_a$ (eV) (above)	$E_a$ (eV) (below)
1	-2.71	0.38
2	-2.20	-1.06
3	-1.56	-0.82
4	-2.22	0.05
5	-2.10	-2.16
6	-1.96	0.09

For platinum atoms, adsorption energies at the grain boundary range between  $-2.71$  and  $0.38$  eV. Again, there is a marked difference between the "above" and "below" adsorption sites. In contrast to the case of gold atoms, however, the platinum atoms preferentially adsorb in the "above" positions, while half of the "below" adsorption positions have positive adsorption energies. Indeed, the adsorption site with the most negative adsorption energy for platinum is also the site where the graphene sheet curves most strongly away from the adsorbate. Also, a considerable negative adsorption energy of  $-2.16$  eV is found for site 5 below the graphene sheet. At this site, the graphene sheet forms a saddle-like shape and thus curves away also from the adsorbate situated below the sheet.

As previously mentioned, we have found no first-principles results regarding the adsorption of gold or platinum atoms on grain boundaries in graphene. However, gold and platinum clusters have been reported to adsorb more strongly to pentagon and heptagon defects<sup>16</sup> as well as to curved graphene surfaces<sup>21,22</sup>. As the grain boundary both contains pentagon and heptagon defects and causes a curvature in the graphene plane, it can be expected that both metals should adsorb more strongly to the grain

boundary than to pristine graphene, and that the "above" adsorption sites should give the most negative segregation energies. This corresponds to the results seen for platinum with the bond-order potential, suggesting that this potential may be useful in the study of metal adsorption on graphene grain boundaries. In contrast, the Lennard-Jones potential used for gold gives the opposite result, with only a minor increase in adsorption strength near the grain boundary and the most stable adsorption sites situated below the graphene grain boundary.

#### IV. CONCLUSIONS

In this study, the adsorption of gold and platinum atoms on pristine graphene and a buckled graphene grain boundary with misorientation angle  $9.4^\circ$  has been investigated. The interaction between gold and carbon has been modeled by a Lennard-Jones potential, while the platinum-carbon interaction has been described using a bond-order potential. Both potentials yield adsorption energies on pristine graphene that are close to those observed in density functional theory studies, although the Lennard-Jones potential predicts the wrong adsorption site as the one with the most negative segregation energy for gold.

For adsorption at the grain boundary, the Lennard-Jones potential predicts that the adsorption energy is at most slightly more negative than that on pristine graphene. As density functional theory studies indicate that both gold and platinum should adsorb more strongly to pentagon and heptagon defects than to pristine graphene, and that the adsorption should also be stronger on a curved graphene surface, this suggests that the Lennard-Jones potential is not suitable for studying adsorption of gold on defects in graphene. Since the Lennard-Jones potential is quite frequently used to describe the interaction between gold and carbon, this also indicates that there is a need to develop a new potential to describe the interaction between these two elements.

In contrast, the bond-order potential used for platinum yields significantly more negative segregation energies at the grain boundary than on pristine graphene, with a maximum difference of 0.8 eV. This demonstrates that the bond-order potential is more suited to studies of the consequences of metal adsorption on grain boundaries in graphene.

#### ACKNOWLEDGEMENTS

We would like to thank Prof. Jari Kinaret for stimulating discussions. We also acknowledge financial support from the Swedish Research Council (VR) and the EU Graphene Flagship (grant no. 604391).

#### REFERENCES

- <sup>1</sup>A. K. Geim, *Science* **324**, 1530 (2009).
- <sup>2</sup>P. Y. Huang, C. S. Ruiz-Vargas, A. M. van der Zande, W. S. Whitney, M. P. Levendorf, J. W. Kevek, S. Garg, J. S. Alden, C. J. Hustedt, Y. Zhu, J. Park, P. L. McEuen, and D. A. Muller, *Nature* **469**, 389 (2011).
- <sup>3</sup>K. Kim, Z. Lee, W. Regan, C. Kisielowski, M. F. Crommie, and A. Zettl, *ACS Nano* **5**, 2142 (2011).
- <sup>4</sup>O. V. Yazyev and Y. P. Chen, *Nature Nanotechnology* **9**, 755 (2014).
- <sup>5</sup>J. Coraux, A. T. N'Diaye, C. Busse, and T. Michely, *Nano Lett* **8**, 565 (2008).
- <sup>6</sup>J. M. Carlsson, L. M. Ghiringhelli, and A. Fasolino, *Phys Rev B* **84**, 165423 (2011).
- <sup>7</sup>T.-H. Liu, G. Gajewski, C.-W. Pao, and C.-C. Chang, *Carbon* **49**, 2306 (2011).
- <sup>8</sup>J. H. Warner, Y. Fan, A. W. Robertson, K. He, E. Yoon, and G. D. Lee, *Nano Lett.* **13**, 4937 (2013).
- <sup>9</sup>A. W. Cummings, D. L. Duong, V. L. Nguyen, D. V. Tuan, J. Kotakoski, J. E. B. Vargas, Y. H. Lee, and S. Roche, *Advanced Materials* **26**, 5079 (2014).
- <sup>10</sup>M. Neek-Amal, R. Asgari, and M. R. R. Tabar, *Nanotechnology* **20**, 135602 (2009).
- <sup>11</sup>J. Wang, L. Zhu, J. Chen, B. Li, and J. T. L. Thong, *Advanced Materials* **25**, 6884 (2013).
- <sup>12</sup>W. D. Luedtke and U. Landman, *Physical Review Letters* **82**, 3835 (1999).
- <sup>13</sup>J. Tersoff, *Phys Rev B* **37**, 6991 (1988).
- <sup>14</sup>J. Tersoff, *Phys Rev Lett* **61**, 2879 (1988).
- <sup>15</sup>K. Albe, K. Nordlund, and R. S. Averback, *Physical Review B* **65**, 195124 (2002).
- <sup>16</sup>Y. Okamoto, *Chemical Physics Letters* **420**, 382 (2006).
- <sup>17</sup>Q. Zhou, Y. Tang, C. Wang, Z. Fu, and H. Zhang, *Comp. Mater. Sci.* **81**, 348 (2014).
- <sup>18</sup>Q. Wang, F. Wang, J. Shang, and Y. Zhou, *J. Phys: Cond. Mat.* **21**, 485506 (2009).
- <sup>19</sup>T. Zhang, L. Zhu, S. Yuan, and J. Wang, *Chem. Phys. Chem.* **14**, 3483 (2013).
- <sup>20</sup>L.-J. Zhou, Z. F. Hou, and L.-M. Wu, *J. Phys. Chem. C* **116**, 21780 (2012).
- <sup>21</sup>A. Staykov, Y. Oishi, and T. Ishihara, *Journal of Physical Chemistry C* **118**, 8907 (2014).
- <sup>22</sup>D. H. Chi, N. T. Cuong, N. A. Tuan, Y.-T. Kim, H. T. Bao, T. Mitani, T. Ozaki, and H. Nagao, *Chemical Physics Letters* **432**, 213 (2006).
- <sup>23</sup>S. J. Plimpton, *J Comput Phys* **117**, 1 (1995), <http://lammps.sandia.gov>.
- <sup>24</sup>L. Lindsay and D. A. Broido, *Phys Rev B* **81**, 205441 (2010).
- <sup>25</sup>D. W. Brenner, *Physical Review B* **42**, 9458 (1990).
- <sup>26</sup>D. W. Brenner, O. A. Shenderova, J. A. Harrison, S. J. Stuart, B. Ni, and S. B. Sinnott, *Journal of Physics: Condensed Matter* **14**, 783 (2002).
- <sup>27</sup>I. Fampiou and A. Ramasubramaniam, *J. Phys. Chem. C* **116**, 6543 (2012).
- <sup>28</sup>E. E. Helgee and A. Isacsson, *Phys. Rev. B* **90**, 045416 (2014).
- <sup>29</sup>W. Humphrey, A. Dalke, and K. Schulten, *J Mol Graphics* **14**, 33 (1996).
- <sup>30</sup>M. Amft, S. Lebegue, O. Eriksson, and N. V. Skorodumova, *J Phys: Condens. Matter* **23**, 395001 (2011).
- <sup>31</sup>K. Okazaki-Maeda, Y. Morikawa, S. Tanaka, and M. Kohyama, *Surface Science* **604**, 144 (2010).